DR1 doped sol-gel planar waveguides for nonlinear devices operating at telecommunications wavelengths

Anne-Claire Le Duff, Michael Canva, Yves Levy, Alain Brun, Frédéric Chaput, Jean-Pierre Boilot, Eric Toussaere

Disperse Red 1-doped solgel planar waveguides for nonlinear optical devices operating at telecommunications wavelengths

Anne-Claire Le Duff, Michael Canva, Yves Lévy, Alain Brun

Laboratoire Charles Fabry de l'Institut d'Optique, Centre National de la Recherche Scientifique, Unité Mixte de Recherche 8501, Institut d'Optique Theorique et Appliquee, Université d'Orsay-Paris XI, BP 147, 91403 Orsay Cedex, France

Vincent Ricci,* Tomas Pliska,† Joachim Meier, George I. Stegeman

School of Optics, Center for Research and Education in Optics and Lasers, University of Central Florida, Orlando, Florida 32816-2700

Frédéric Chaput and Jean-Pierre Boilot

Laboratoire de Physique de la Matière Condensée, Centre National de la Recherche Scientifique, Unité Mixte de Recherche 7643, École Polytechnique, Palaiseau, France

Eric Toussaere

Laboratoire de Photonique Quantique et Moléculaire, Centre National de la Recherche Scientifique, Unité Mixte de Recherche 8537, École Normale Supérieure, Cachan, France

Received November 2, 2000; revised manuscript received January 19, 2001

We report on linear and nonlinear optical properties of Disperse Red 1-doped solgel waveguides. The refractive-index and optical-propagation losses of the guiding layer were measured between 0.756 μm and 1.64 μm. The spectral broadening of the chromophore charge-transfer transition in the visible is modeled with a Voigt-profile function. In the telecommunications window the attenuation is dominated by the overtones of the O—H bonds vibration bands. The nonlinear optical coefficients were measured at different poling strengths with the Maker-fringe method. The nonlinear coefficient d_{33} was found to be 4.5 pm V^{-1} at 1.58 μm for a poling field of 60 V μm^{-1}. © 2001 Optical Society of America

OCIS codes: 130.0130, 160.6060, 190.4400, 300.1300, 190.2620.

1. INTRODUCTION

Organic molecules can exhibit large optical nonlinearities. They have been incorporated in various materials systems, e.g., polymers, organic single crystals, Langmuir–Blodgett films, and liquid crystals. In the past years, most of the research has focused on poled organic polymers, with some remarkable achievements such as high-bandwidth electro-optic modulators[1] and modal dispersion phase-matched second-harmonic generation at 1.55 μm.[2]

Meanwhile, solgel materials, the hybrid organic–inorganic counterparts of all-organic polymers, are receiving increasing attention as a chemically and mechanically more robust alternative for nonlinear applications in integrated optics.[3] The low-temperature solgel process provides a highly convenient route for preparing uniform high-optical-quality thin films (or monoliths) of oxide glass. Like all-organic polymers, solgel materials can be tailored to meet specific requirements (such as refractive index and conductivity), and organic chromophores can be incorporated in the solgel matrix. Quadratic nonlinear coefficients d_{33} up to 17 pm V^{-1} at 1.542 μm have been demonstrated.[4]

Many chromophore classes used in nonlinear optics exhibit an increasing hyperpolarizability with a redshift of the ultraviolet–visible charge-transfer transition.[5] Therefore in most cases the transparency properties at the second-harmonic wavelength become a critical issue. The linear-attenuation coefficient at the second harmonic depends on both the position of the absorption peak and the slope of the absorption edge,[6] and careful modeling of the absorption spectrum in this wavelength region is necessary. Otomo *et al.*[7] have discussed the effect of spectral broadening on second-harmonic generation in 4-dimethylamino-4′-nitrostilbene side-chain polymer. Similarly, Pliska and colleagues have considered several nonlinear polymer systems: it appeared that DR1 offers a good compromise between nonlinearity and linear absorption.[8]

In this paper we report on Disperse Red 1 (DR1)-doped solgel waveguide fabrication and on a number of optical properties of the samples. Absorption and optical-

0740-3224/2001/121827-05$15.00

propagation-loss measurements were performed in the visible and in the near-infrared (NIR) range up to 1.64 μm. The spectrum was modeled with an inhomogeneously broadened Voigt profile. The nonlinear optical coefficients were measured with a Maker-fringes setup. The potential of the material for second-harmonic generation at 1.55 μm is examined. Finally, the DR1-doped solgel under investigation is compared with the nonlinear side-chain polymer Disperse Red 1–poly(methyl methacrylate) (DR1-PMMA) from International Business Machines.

2. LINEAR CHARACTERIZATION

The solgel process was used to prepare hybrid thin films integrating both push–pull DR1 molecules and carbazole units in a rigid backbone of a silica-based matrix. The carbazole molecules act as spacer entities in the highly concentrated DR1-doped matrix. The solution was synthesized according to an experimental procedure previously described.[9] Appropriately functionalized triethoxysilane monomers were copolymerized with the tetraethoxysilane (TEOS) cross-linking agent in a mutual cosolvent. Figure 1 gives a schematic representation of the hybrid network as well as the chemical reaction. SiK–DR1–TEOS films were then spin coated on various substrates and cured for 12 h at 120 °C. The layer thickness depends on deposition conditions, i.e., viscosity and rotation speed.

The refractive index of the SiK–DR1–TEOS material (Fig. 2) was measured by ellipsometry. The results were cross checked with attenuated-total-reflection experiments on two different samples. With a grating-coupling method we also verified that the curing time does not affect too much the refractive index of the material: the difference between cured and uncured samples remains 3×10^{-3}.

Because the absorption in the visible and the NIR is dominated by a single charge-transfer line, it is reasonable to fit the dispersion curve to a one-oscillator Sellmeier dispersion formula, given by

$$n^2(\omega) - 1 = A_0 + \frac{A_1}{\omega^2 - \omega_0^2}, \tag{1}$$

where A_0 is the dispersion-free contribution from the other oscillators. A_1 represents the oscillator strength, and ω_0 is the resonant frequency of the oscillator. The fitting results are the following: $A_0 = 1.4215$, $A_1 = 2.216 \times 10^{30}\,\mathrm{rad^2\,s^{-2}}$, and $\omega_0 = 3.823 \times 10^{15}\,\mathrm{rad\,s^{-1}}$. The corresponding curve is displayed in Fig. 2. The resonant part of the Sellmeier equation can be correlated to the zero-frequency molecular polarizability α_0.[10] Assuming a local-field correction factor given by the Lorentz approximation, the calculation gives $\alpha_0 = 5.9 \pm 2.0 \times 10^{-39}\,\mathrm{C\,m^2\,V^{-1}}$ ($5.3 \pm 1.6 \times 10^{-23}$ esu). The number density of active molecules is known with only 30% accuracy, which translates directly into the quoted uncertainty in α_0. Nevertheless, the calculation is in good agreement with a value previously measured in *p*-dioxane solvent (3.8×10^{-23} esu).[5] From this we conclude that DR1 molecules, albeit tightly attached to the cross-linked solgel matrix, retain their intrinsic molecular properties.

The absorption spectrum of SiK–DR1–TEOS is shown in Fig. 3. For wavelengths between 0.4 and 0.65 μm, the absorption was measured in transmission with a Cary spectrophotometer and use of a 2-μm-thick film [Fig. 3(a)]. To estimate the absorption in the 0.7–1.65-μm region, where transmission spectroscopy through a thin film does not provide sufficient resolution, we measured the optical loss in an unpoled SiK–DR1–TEOS slab waveguide. The optical-propagation-loss measurements, displayed in an expanded view in Fig. 3(b), were performed in 2-μm-thick solgel films spin coated on thermally oxidized silicon wafers [inset of Fig. 3(b)]. The low-refractive-index SiO_2 buffer layer is 2.6 μm thick to ensure negligible tunneling losses. The light was coupled into the solgel waveguide with a prism coupler. The propagation-loss coefficient was determined by imaging the light streak in a CCD camera. Since the scattered light exhibits an exponential decay owing to both scattering and absorption in the waveguide, the results provide an upper limit of the absorption coefficient. The attenuation coefficient at 0.78 μm is $1.0 \pm 0.3\,\mathrm{cm^{-1}}$. This result is in good agreement with the previously published

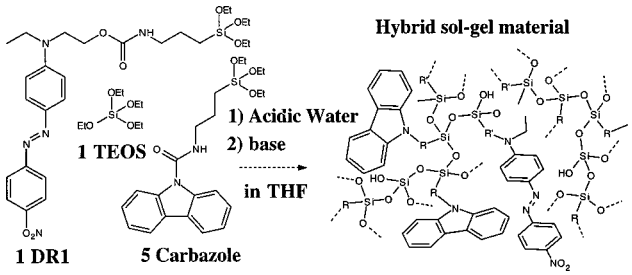

Fig. 1. Schematic representation of the hybrid film synthesis from silane-modified monomers. The three monomers are dissolved in tetrahydrofurane. Acidic water is added to the solution to hydrolyze all the ethoxy groups. After complete hydrolysis, a base is added to promote the condensation of the released silanols into siloxane bonds.

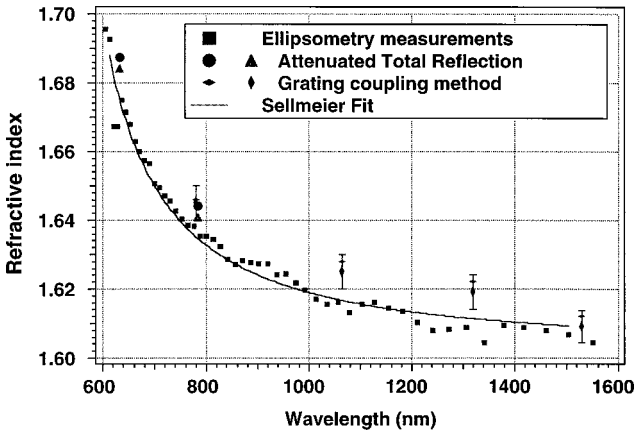

Fig. 2. Refractive index of SiK–DR1–TEOS material in the visible–NIR. The ellipsometry measurements (filled squares) were performed on 2.5-μm-thick solgel films spin coated on silicon substrates. Two other samples were tested in an attenuated-total-reflection experiment (filled circles and triangles). A grating-coupling method was used to check the influence of the curing (tall diamond, noncured; short diamond, cured). The ellipsometry data are fitted according to the Sellmeier model.

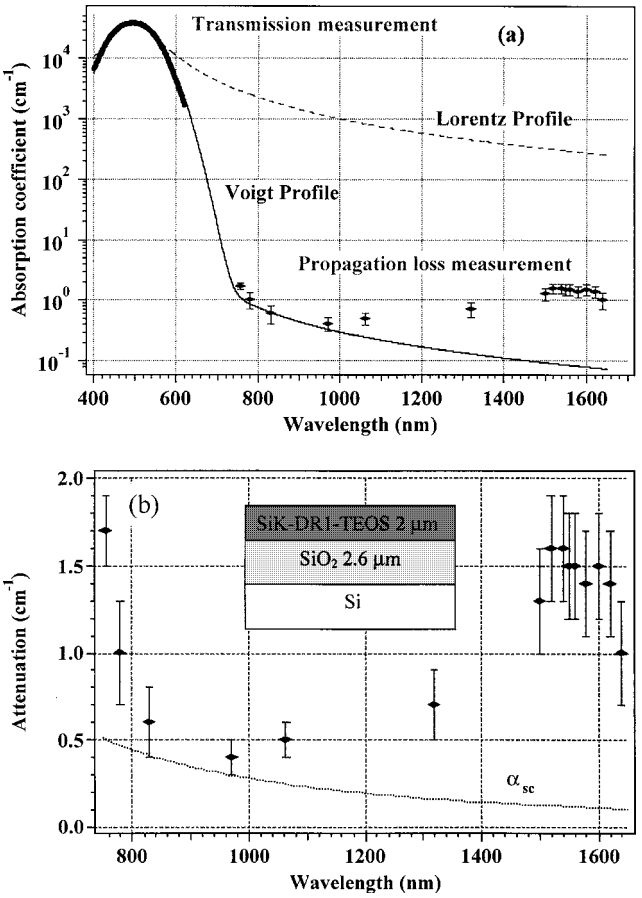

Fig. 3. (a) Absorption spectrum of SiK–DR1–TEOS solgel. The data between 0.4 and 0.65 μm were obtained by transmission spectroscopy with a spectrophotometer. The optical propagation losses are also presented (diamonds). The absorption spectrum is fitted with both a Voigt (solid curve) and a Lorentz (dashed curve) profile modeling the inhomogeneous and the homogeneous broadening, respectively. (b) Expanded view of the IR waveguide loss of a planar SiK–DR1–TEOS of 2-μm thickness on SiO_2. The scattering losses α_{sc} are calculated assuming a film roughness of 5 nm. The inset shows the waveguide structure used for the propagation-loss measurement.

values of 0.3 to 0.7 cm^{-1} for the all-organic side-chain polymer DR1–PMMA.[8] The scattering losses α_{sc} [dashed curve in Fig. 3(b)] are dominant between 0.8 and 1.1 μm. In the telecommunication windows (1.3 and 1.55 μm) the absorption spectrum is dominated by the overtones of the O—H bond vibration bands.[11] At 1.55 μm the absorption coefficient is $1.5 \pm 0.3\,\mathrm{cm}^{-1}$. While the fundamental vibration mode of the network bond Si–O–Si peaks around $1090\,\mathrm{cm}^{-1}$ ($\lambda = 9.2\,\mu$m) and is unlikely to generate absorption losses in the NIR, the O—H vibration band is centered around $3465\,\mathrm{cm}^{-1}$ ($\lambda = 2.9\,\mu$m). Therefore the first overtone of the O—H vibration mode falls right into the telecommunications windows. In comparison, in an optical fiber, the high-temperature process limits the O—H bond content, yielding very small losses at 1.55 μm. A thermal treatment at high temperature is impossible in our solgel material owing to the presence of organic compounds in the solgel matrix. However, some effects of the curing process are currently under investigation, and one can expect a reduction of propagation loss in the telecommunications window in the near future.

Those high losses at the fundamental wavelength of 1.55 μm will severely limit the second-harmonic conversion efficiency of a waveguide device. Clearly, further improvement in material technology is necessary to reduce the absorption. A humidity-controlled environment could probably reduce the expected losses in the telecommunications window. Another strategy would be the development of a matrix that involves bifunctionalized alkoxide precursors instead of the triethoxysilane monomers. A similar approach has been followed in all-organic polymers: there the C—H vibration overtones are a considerable source of loss in the IR[12] that can be reduced by replacing the hydrogen by, e.g., fluorine or chlorine.

3. MODELING AND DISCUSSION

The linear absorption of the hybrid solgel material under investigation is dominated by two different excitation mechanisms. In the UV–visible part of the spectrum the electronic transitions are responsible for strong absorption bands, whereas for wavelengths >1.3 μm, most of the absorption is due to much weaker vibration overtones of O—H bonds.

Far from any electronic resonance, the absorption coefficient $\alpha(\omega)$ is calculated from the following relation:

$$\alpha(\omega) = \frac{\omega}{cn(\omega)}\,\mathrm{Im}[\chi^{(1)}(\omega)], \tag{2}$$

where $\chi^{(1)}(\omega)$ is the linear susceptibility of the material at optical frequencies. A two-level model involving a transition from the ground state to the first excited state can be used to describe the dominant contribution to the attenuation coefficient near the peak absorption wavelength. In this approach the linear susceptibility $\chi^{(1)} \times (\omega)$ is given by

$$\chi^{(1)}(\omega) = \frac{Nf^{\omega}\Theta}{\varepsilon_0\hbar}|\mu_{01}|^2\left(\frac{1}{\omega_{01} - \omega + j\Gamma_{01}/2} + \frac{1}{\omega_{01} + \omega - j\Gamma_{01}/2}\right), \tag{3}$$

where N is the number density of dipoles, f^{ω} is the local-field correction factor, and Θ is the molecular-orientation factor ($\Theta = 1/3$ for randomly oriented dipoles). Γ_{01} and μ_{01} represent the homogenous broadening and the dipole moment of the charge-transfer transition, respectively. The dashed curve in Fig. 3(a) represents a fit of the absorption data according to Eq. (3). The fitted parameters are listed in Table 1. In the NIR this Lorentz profile

Table 1. Fitting Parameters of SiK–DR1–TEOS Absorption Profiles

Parameters	Lorentz Profile	Voigt Profile
$N\lvert\mu_{01}\rvert^2$ (C m^{-1})	$1.6 \pm 0.2 \times 10^{-31}$	$1.7 \pm 0.2 \times 10^{-31}$
Γ_{01} (rad s^{-1})	$590 \pm 30 \times 10^{12}$	$0.40 \pm 0.05 \times 10^{12}$
$\Delta\omega_{01}$ (rad s^{-1})	Not applicable	$560 \pm 30 \times 10^{12}$
ζ	Not applicable	0.38 ± 0.05

grossly overestimates the absorption by several orders of magnitude.

This discrepancy can be resolved by introducing vibrational contributions into the model.[13] For the DR1 molecule (see the chemical structure in Fig. 1), the stretching mode of the N=N double bond and the breathing mode of the phenyl ring occur around 1380 cm^{-1} (7.32 μm)[14] and 1321 cm^{-1} (7.6 μm), respectively.[13] Such vibration transitions are expected to broaden the chromophore charge-transfer transition in the visible. Then, to reproduce the details of the absorption bands further away from resonance, an inhomogeneously broadened linear susceptibility is more appropriate.[15] In this approach, $\chi^{(1)}(\omega)$ is given by[7]

$$\chi^{(1)}(\omega) = \frac{\sqrt{\pi} N f^{\omega} \Theta}{\varepsilon_0 \hbar} |\mu_{01}|^2 \times \int_{-\infty}^{+\infty} \left(\frac{1}{\omega'_{01} - \omega + j\Gamma_{01}/2} + \frac{1}{\omega'_{01} + \omega - j\Gamma_{01}/2} \right) g_{01}(\omega'_{01} - \omega_{01}) \times d(\omega'_{01} - \omega_{01}), \quad (4)$$

where the inhomogeneous broadening is described by the asymmetric Gaussian function $g_{01}(\omega'_{01} - \omega_{01})$:

$$g_{01}(\omega'_{01} - \omega_{01}) = \frac{1}{\pi \Delta \omega'_{01}} \exp\left[-\left(\frac{\omega'_{01} - \omega_{01}}{\Delta \omega'_{01}} \right) \right], \quad (5)$$

where the asymmetric linewidth is defined as

$$\Delta \omega'_{01} = \frac{\Delta \omega_{01}}{1 - \zeta + \zeta \left(\frac{\omega_{01}}{\omega} \right)^2}. \quad (6)$$

$\Delta \omega_{01}$ is the inhomogeneous broadening and ζ is the asymmetry parameter. Then, the line shape of the charge-transfer transition is given by the so-called Voigt profile, i.e., the convolution of the asymmetric Gaussian function dominating near the absorption peak and a Lorentzian function prevailing in the tail of the spectrum. In this approach the contribution from resonances at higher frequencies is represented by a constant $\chi_b^{(1)}$.

Fitting the measured absorption spectrum to the inhomogeneously broadened function was performed with Labview and Matlab software. The absorption spectrum of SiK–DR1–TEOS was modeled with Eq. (4) to find the unknown parameters $N|\mu_{01}|^2$, $\Delta \omega_{01}$, Γ_{01}, and ζ. The Voigt profile is represented in Fig. 3(a), and the corresponding parameters are listed in Table 1. Here the second-harmonic wavelength (0.78 μm) falls in the Gaussian part of the absorption line. This fit reproduces the measurement up to ~1 μm, well above the second-harmonic wavelength. It does not describe the absorption further in the IR, where a different absorption mechanism is dominant. The inhomogeneous broadening of the charge-transfer transition of the DR1 in the solgel material is comparable to previously published data on the DR1-PMMA polymer material.[8] Broadening mechanisms are then supposed to be very similar in both materials.

4. NONLINEAR OPTICAL CHARACTERIZATION

Solgel films exhibit a random orientation of the chromophores after deposition. An electrical poling process is necessary to break the natural centrosymmetry and generate quadratic nonlinear properties.

For nonlinear optical characterization, 2.5-μm-thick films were spin coated onto indium-tin-oxide-coated glass substrates. Approximately 150-nm-thick Al electrodes were deposited on top of the films by thermal evaporation. Poling was performed in a furnace at atmospheric pressure. Once the sample reached the poling temperature of 120 °C, a voltage was applied between the bottom indium tin oxide and top Al electrodes. The voltage was carefully ramped at a rate of ~10 $V\,min^{-1}$ up to typically some tens of $V\,\mu m^{-1}$. The samples were kept at the poling temperature for ~2 h. Then, they were slowly cooled to room temperature at a rate of ~0.5 °C min^{-1} with the voltage still applied. Afterwards, the top electrode was etched off with a mixture of phosphoric, acetic, and nitric acid before further processing.

A standard Maker-fringes setup was used to measure the nonlinear coefficients of the poled solgel films. The calibration was performed with a y-cut quartz plate with a nonlinear coefficient $d_{11} = 0.29\,pm\,V^{-1}$ at 1.58 μm.[16] The 1.58-μm fundamental radiation was generated by Raman shifting the output of a frequency-doubled (0.532-μm) Q-switched Nd:YAG laser (pulse duration 10 ns) in a hydrogen cell. Typical pulse energies at 1.58 μm incident upon the sample were of the order of 10 μJ. The transmitted fundamental beam was blocked with a set of density filters, while the second-harmonic signal passed through a spectrometer before detection with a photomultiplier tube.

The measured nonlinear coefficient d_{33} of SiK–DR1–TEOS films is presented in Fig. 4 as a function of the external poling field. We measured $d_{33} = 4.5 \pm 0.4\,pm\,V^{-1}$ at 1.58 μm for a poling field of 60 $V\,\mu m^{-1}$.

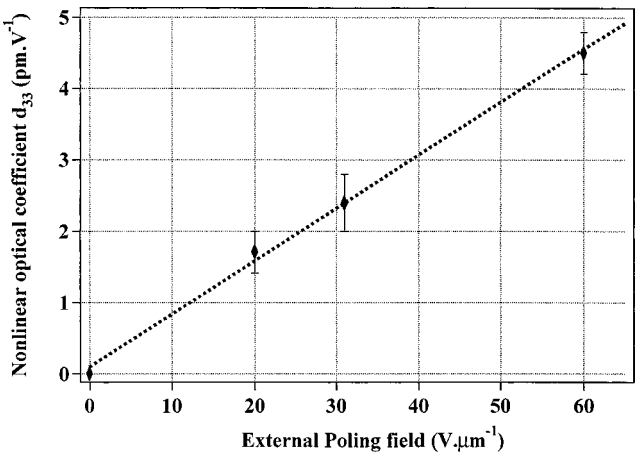

Fig. 4. Nonlinear coefficient d_{33} as a function of the poling strength. The measurements were performed at 1.58 μm.

These measured values are consistent with the nonlinear quadratic coefficient of the DR1–PMMA.[8] The poling field was limited by the poling current. Indeed, the poling current increased strongly above 80–90 $V\,\mu m^{-1}$, and electrical breakdown was likely to occur. This behavior is attributed to ionic species in the solgel matrix. For DR1–PMMA polymer systems, fields up to 150 $V\,\mu m^{-1}$ could be applied on samples of the same thickness.[8]

5. CONCLUSION

In conclusion, we found that our solgel system exhibits similar nonlinearity and absorption loss at the harmonic wavelength as the corresponding side-chain polymer DR1–PMMA. However, high losses were measured within the telecommunication windows. They are attributed to the overtones of O—H vibration bands. Finally, taking our measured values of $\alpha_\omega = 1.5\,cm^{-1}$, $\alpha_{2_\omega} = 1.0\,cm^{-1}$, and $d_{33} = 4.5\,pm\,V^{-1}$, and assuming a waveguide with an effective cross section of 10 μm^2 (typical value for annealed proton-exchanged lithium niobate waveguide) and an optimized length of 1.1 cm, we calculate a normalized conversion efficiency of 10% W^{-1} for second-harmonic generation at 1.55 μm. Clearly, to increase this figure, further improvement of material processing is necessary to reduce the loss at the fundamental and to allow a higher poling field. Our future study will be directed accordingly.

ACKNOWLEDGMENTS

This research is supported by a Plan Pluri-Formations French grant and by National Science Foundation–Centre National de la Recherche Scientifique U.S.–French bilateral collaboration funds. T. Pliska wishes to acknowledge financial support by the Swiss National Science Foundation. A.-C. Le Duff thanks A. Otomo (Kansai Advanced Research Center, Kobe, Japan) for useful discussion.

*Present address: Corning, Inc., New York 14830.

†Present address: Nortel Neworks AG, Binzstrasse 17, CH-8045 Zurich, Switzerland.

REFERENCES

1. Y. Shi, C. Zhang, H. Zhang, J. H. Betchel, L. R. Dalton, B. H. Robinson, and W. H. Steier, "Low (Sub-1-Volt) halfwave voltage polymeric electro-optic modulators achieved by controlling chromophore shape," Science **288**, 119–122 (2000).
2. M. Jäger, G. I. Stegeman, S. Yilmaz, W. Wirges, W. Brinker, S. Bauer-Gogonea, S. Bauer, M. Ahlheim, M. Stähelin, B. Zysset, F. Lehr, M. Diemeer, and M. C. Flipse, "Poling and characterization of polymer waveguides for modal dispersion phase-matched second-harmonic generation," J. Opt. Soc. Am. B **15**, 781–788 (1998).
3. M. P. Andrews, "An overview of sol-gel guest-host materials chemistry for optical devices," in *Integrated Optics Devices: Potential for Commercialization*, S. Nafaji and M. N. Armenise, eds., Proc. SPIE **2997**, 48–59 (1997).
4. G. H. Hsiue, R. H. Lee, and R. J. Jeng, "All sol-gel organic-inorganic nonlinear optical materials based on melamines and an alkoxysilane dye," Polymer **40**, 6417–6428 (1999).
5. L. T. Cheng, W. Tam, S. H. Stevenson, G. R. Meredith, G. Rikken, and S. R. Marder, "Experimental investigations of organic molecular nonlinear optical polarizabilities. 1. Methods and results on benzene and stilbene derivatives," J. Phys. Chem. **95**, 10631–10643 (1991).
6. A. C. Le Duff, V. Ricci, T. Pliska, M. Canva, G. Stegeman, K. P. Chan, and R. Twieg, "Importance of chromophore environment on the near-infrared absorption of polymeric waveguides," Appl. Opt. **39**, 947–953 (2000).
7. A. Otomo, M. Jäger, G. Stegeman, M. C. Flipse, and M. Diemer, "Key trade-off for second harmonic generation in poled polymers," Appl. Phys. Lett. **69**, 1991–1993 (1996).
8. T. Pliska, W. R. Cho, J. Meier, A. C. Le Duff, V. Ricci, A. Otomo, M. Canva, G. Stegeman, P. Raimond, and F. Kajzar, "Comparative properties of nonlinear optical polymers for guided-wave second-harmonic generation at telecommunication wavelengths," J. Opt. Soc. Am. B **17**, 1554–1564 (2000).
9. F. Chaput, D. Riehl, J. P. Boilot, T. Gacoin, M. Canva, Y. Levy, and A. Brun, "Photorefractive sol-gel materials," in *Better Ceramics Through Chemistry VII*, Mater. Res. Soc. Symp. Proc. **435**, 583–588 (1996).
10. M. Born and E. Wolf, *Principles of Optics*, 6th ed. (Cambridge University, London, 1992), pp. 92–97.
11. M. A. Mondragón, V. M. Castaño, J. Garcia, and S. Téllez, "Vibrational analysis of $Si(OC_2H_5)_4$ and spectroscopic studies on the formation of glasses via silica gels," Vib. Spectrosc. **9**, 293–304 (1995).
12. A. Skumanich, M. Jurich, and J. D. Swalen, "Absorption and scattering in nonlinear polymeric systems," Appl. Phys. Lett. **62**, 446–448 (1993).
13. J. Cornil, D. Beljonne, S. J. Martin, D. D. C. Bradley, T. Hagler, M. Cha, W. E. Torruellas, G. Stegeman, and J. L. Brédas, "Vibronic contributions in frequency-dependent linear and nonlinear optical processes: a joint experimental and theoretical study," in *Photoactive Organic Material,* F. Kajzar and V. M. Agranovich, eds., Proc. NATO Adv. Res. Workshop **9**, 17–32 (1995).
14. Y. Lévy, F. Chaput, D. Rhiel, and J. P. Boilot, "Nonlinear optical properties of stable sol-gel systems," in *Photoactive Organic Material*, F. Kajzas and V. M. Agranovich, eds., Proc. NATO Adv. Res. Workshop **9**, 247–262 (1995).
15. E. Toussaere, "*Polymères électro-optiques pour l'optique non linéaire: caractérisation optique et modèles statistiques*," Ph.D. dissertation (Université Paris-Sud, France, 1993).
16. D. A. Roberts, "Simplified characterization of uniaxial and biaxial nonlinear optical crystals: a plea for standardization of nomenclature and conventions," IEEE J. Quantum Electron. **28**, 2057–2074 (1992).